Southern Hemisphere Early Cretaceous (Valanginian-Early Barremian) carbon and oxygen isotope curves from the Neuquén Basin, Argentina

María B. Aguirre-Urreta [a,*], Gregory D. Price [b], Alastair H. Ruffell [c], Darío G. Lazo [a], Robert M. Kalin [d], Neil Ogle [d], Peter F. Rawson [e,f]

[a] *Departamento de Ciencias Geológicas, Universidad de Buenos Aires, Ciudad Universitaria, 1428 Buenos Aires, Argentina*
[b] *School of Earth, Ocean and Environmental Sciences, University of Plymouth, Drakes Circus, Plymouth, PL4 1PM, UK*
[c] *School of Geography, Queen's University, Belfast, Northern Ireland, BT7 INN, UK*
[d] *School of Planning, Architecture and Civil Engineering, Queen's University, Belfast, Northern Ireland, BT7 INN, UK*
[e] *Department of Earth Sciences, University College London, Gower Street, London, WC1E 6BT, UK*
[f] *Centre for Environmental and Marine Sciences, University of Hull (Scarborough Campus), Filey Road, Scarborough, YO11 3AZ, UK*

Abstract

The first carbon and oxygen isotope curves for the Valanginian to Early Barremian (Early Cretaceous) interval obtained from outcrops in the Southern Hemisphere are presented. They were obtained from well-dated (by ammonites) sediments from the Neuquén Basin, Argentina. Measurements were acquired by the innovative method of analysing fossil oyster laminae. The occurrence of the well-established mid-Valanginian positive carbon isotope excursion is documented, while less well-marked positive events may also correlate with peaks identified in the well-known successions of SE France. The mid-Valanginian positive carbon isotope event in the Neuquén Basin is possibly associated with organic-rich sediments. A similar relationship is seen in the European Alps and in oceanic cores in some areas of the world.
© 2007 Elsevier Ltd. All rights reserved.

Keywords: Argentina; Neuquén Basin; Carbon isotopes; Oxygen isotopes; Early Cretaceous

1. Introduction

The Valanginian positive carbon isotope event is widely recorded in marine carbonates and has been postulated to represent the onset of the Cretaceous greenhouse earth (Lini et al., 1992). These greenhouse conditions have been linked to the Paraná-Etendeka continental flood-basalts (Channell et al., 1993; Courtillot et al., 1999; Gröcke et al., 2005) and related carbonate-platform drowning episodes (Föllmi et al., 1994).

The initial aims of our study were: to produce the first outcrop record of Valanginian to Early Barremian (Early Cretaceous) carbon and oxygen isotope curves from a Southern Hemisphere basin (the Neuquén Basin in west-central Argentina); to determine whether the widespread mid-Valanginian positive carbon isotope event was represented there; and to compare changes in $\delta^{13}C$ with proxy palaeotemperatures obtained from the $\delta^{18}O$ curve presented here. Whilst the first two aims were achieved, we were unable to obtain reliable proxy temperatures from the $\delta^{18}O$ analysis because changes in salinity dominated the signal in our analysed material (oyster shells). Instead, we have used the $\delta^{18}O$ data in combination with palaeoecological evidence, to estimate possible water salinity variation within the basin. Oxygen isotope data show that palaeosalinity in the Neuquén Basin underwent significant fluctuations from Early Valanginian to Early Barremian times, with a clear tendency to increase from brachyhaline to euhaline and roughly hyperhaline conditions (Lazo et al., in press).

Our ultimate aim was to draw attention to, and critically examine, the linking of the mid-Valanginian carbon isotope excursion with the supposedly contemporaneous eruption of the Paraná-Etendeka basalts (e.g., Channell et al., 1993; Erba et al., 2004). The Neuquén Basin is one of the marine

* Corresponding author.

  E-mail address: aguirre@gl.fcen.uba.ar (M.B. Aguirre-Urreta).

basins nearest to this major volcanic province and has the best documented Early Cretaceous records. The results are discussed below.

2. Geological setting

2.1. The Neuquén Basin

The Neuquén Basin, in west-central Argentina (32°–40°S; Fig. 1), is a major Mesozoic to Neogene depocentre, and is one of the few Southern Hemisphere basins to have a good marine record from latest Jurassic to mid Early Cretaceous (Barremian) times. During that interval, the area formed a back-arc basin linked to the Pacific Ocean on its western margin through a volcanic island arc. Its depositional evolution was controlled by a combination of eustasy and local tectonics (Legarreta and Gulisano, 1989). The depositional surface was generally of low gradient, causing large embayments to form during episodes of relative sea-level rise (Legarreta and Gulisano, 1989). The Valanginian-Early Barremian succession is composed of siliciclastics and carbonates of predominantly marine origin, though some non-marine sediments also occur. Thick and laterally continuous outcrops and an abundant fossil record make the Neuquén Basin an excellent site for stratigraphical, palaeontological and geochemical studies. Its importance is further enhanced because the succession includes several economically-important hydrocarbon source, seal and reservoir rocks (Uliana and Legarreta, 1993).

2.2. The stratigraphic succession

The samples analysed here are from three formations of the Mendoza Group, the Vaca Muerta, Mulichinco and Agrio formations (Fig. 2). A refined ammonite biostratigraphy indicates a Tithonian to Early Barremian age (Aguirre-Urreta and Rawson, 1997; Aguirre-Urreta et al., 2005). The Vaca Muerta Formation (Tithonian-Lower Valanginian) is a monotonous succession of finely-stratified black and dark grey shales and lithographic lime-mudstones, 200–1700 m thick. It is interpreted as a restricted inner basin succession, deposited during low benthic oxygen levels (Legarreta and Gulisano, 1989; Doyle et al., 2005). The Mulichinco Formation (spanning the Lower/Upper Valanginian boundary) comprises non-marine conglomerates and sandstones that grade into marine sandstones and shales towards the north, reaching 200 m maximum thickness. The boundary with the overlying Agrio Formation (Upper Valanginian-Lower Barremian) is diachronous, becoming younger southward and eastward. The Agrio Formation (1600 m maximum) is divided into three members, the Pilmatué, Avilé and Agua de la Mula Members. The formation comprises mainly marine shales, sandstones and limestones, but the Avilé Member is a thin fluvial and aeolian sandstone that marks a mid-Hauterivian fall in sea level (e.g., Spalletti et al., 2001; Veiga et al., 2002).
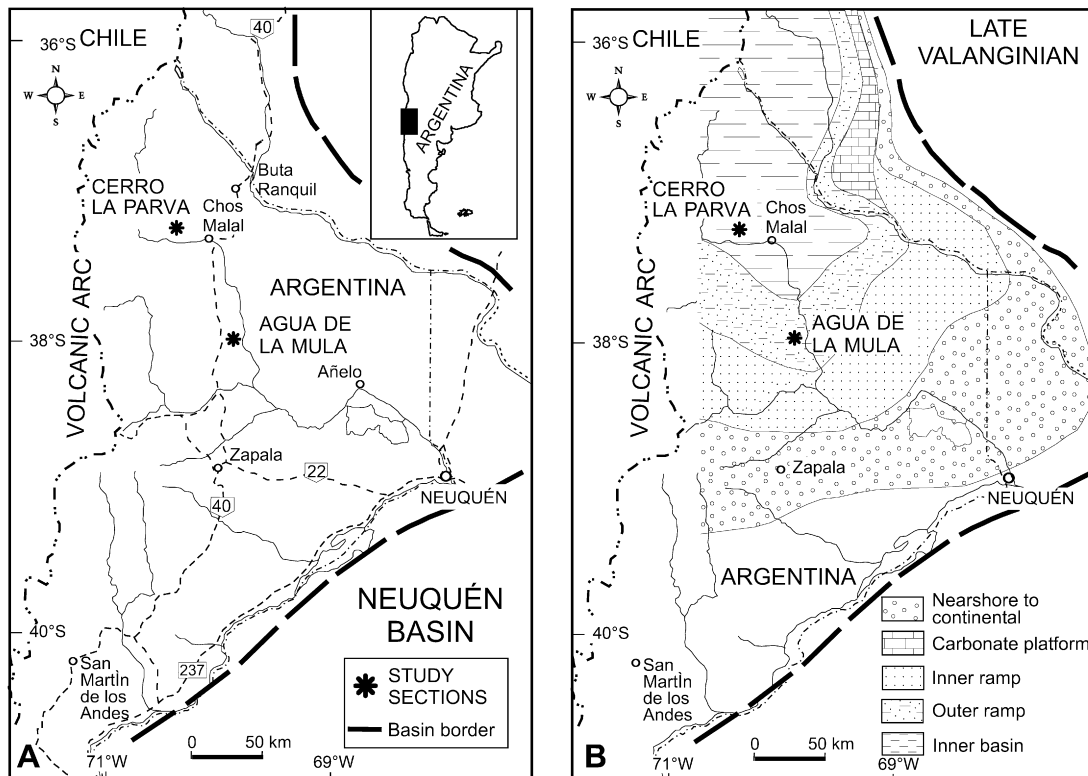

Fig. 1. A, The Neuquén Basin in west-central Argentina, with location of the studied localities Cerro La Parva and Agua de la Mula. B, Palaeogeographic map of the basin during Late Valanginian times (modified from Legarreta and Uliana, 1991).
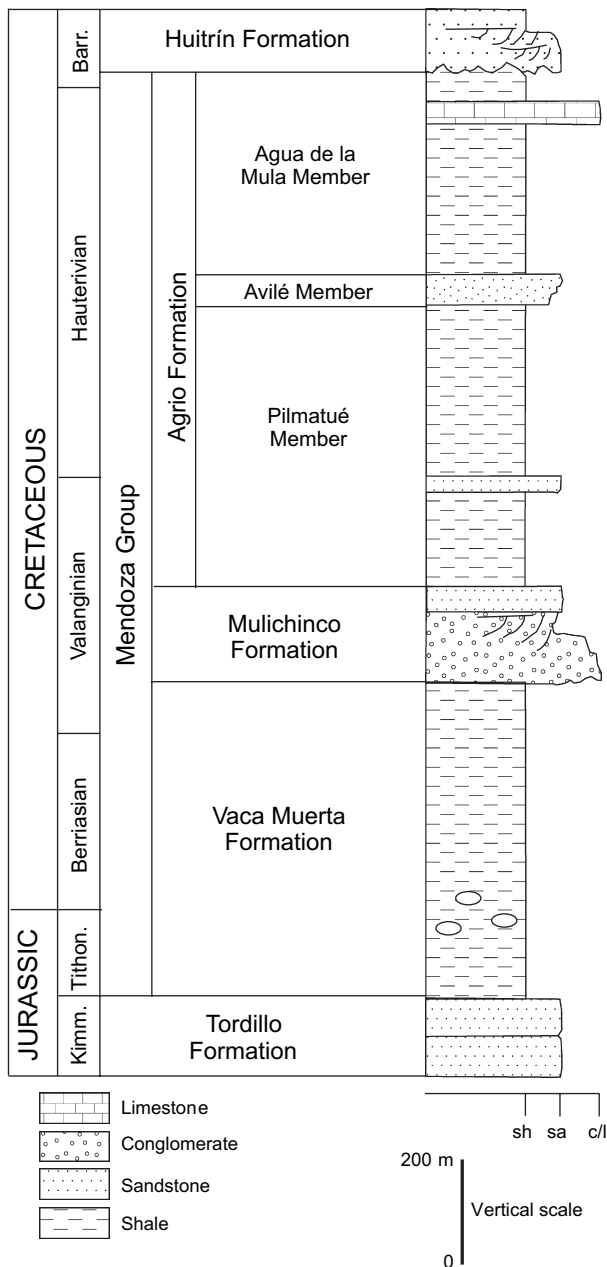
Fig. 2. Lithostratigraphic division of the Mendoza Group.

3. Material and methods

3.1. Material

Belemnites are commonly used to provide biogenic calcite for carbon and oxygen isotope studies (e.g., Price et al., 2000; van de Schootbrugge et al., 2000), but they are completely missing from the Valanginian to Barremian successions of the Neuquén Basin. Instead, we have analysed oyster-shell material to construct an isotope stratigraphy. This is the first time, to our knowledge, that oysters have been utilised in isolation, although the isotopic composition of oysters has been exploited for palaeoenvironmental and palaeoceanographic studies (e.g., Jones et al., 1994; Cochran et al., 2003; Holmden

and Hudson, 2003), while Steuber and Rauch (2005) have recently produced a carbon isotope curve from another bivalve group, the rudists.

For the isotopic analysis, samples of oyster shells of 2 cm long were collected bed by bed at Cerro La Parva and Agua de la Mula. Oyster samples were collected *in situ* from 52 levels: three in the Vaca Muerta Formation, three in the Mulichinco Formation, and 46 in the Agrio Formation. Sampling was subject to the presence of oysters and thus samples are unevenly distributed throughout the units studied. Before sampling, the shell material was inspected with a hand lens and discarded if any alteration was suspected. From several levels, more than one sample of oyster was collected, and also each oyster was divided into between three and six sub-samples when processing (see below, and Tables 1–3).

The sampled oysters belong to the genera *Aetostreon* Bayle and *Amphidonte* (*Ceratostreon*) Bayle of the Family Gryphaeidae (see Cooper, 1995). *Aetostreon* forms a group of very inequivalved, very thick-shelled oysters, whose adults were mainly soft-bottom recliners that reached a large size (22 cm maximum height). *Aetostreon* are common within the units studied. These oysters peak in abundance in the *Olcostephanus (O.) atherstoni* and '*Neocomites*' sp. ammonite Subzones and *Crioceratites diamantensis* ammonite Zone.

Amphidonte (*Ceratostreon*) includes a group of small oysters (9 cm maximum height) with inequivalved valves and chomata. These oysters are comma-shaped, and have a large attachment area and conspicuous radial ribs. They commonly encrust molluscs, corals, serpulids and carbonate concretions. They are recorded throughout the three studied units in all ammonite zones, and are, in fact, one of the most common bivalves in the Early Cretaceous of the Neuquén Basin. They form occasional mass aggregations immersed in mud, especially within the *O.* (*O.*) *atherstoni* and *O.* (*O.*) *laticosta* ammonite Subzones.

Both groups of oysters were collected from 52 levels ranging from the Lower Valanginian to the Lower Barremian at two different localities in the Neuquén Basin: Cerro La Parva and Agua de la Mula (Fig. 1). Cerro La Parva is located 23 km north-west of Chos Malal. The section is composed of the upper part of the Vaca Muerta Formation, the Mulichinco Formation and the lower part of the Pilmatué (formerly Lower) Member of the Agrio Formation. Agua de la Mula (Cerro Mula) is located 90 km south of Chos Malal, 3 km east of the national road 40. It has excellent exposures of the top of the Mulichinco Formation and the three members of the Agrio Formation.

3.2. Petrography

Standard thin-sections of oysters were examined by petrographic methods and cathodoluminescence (CL). Luminescence signatures are caused by trace elements and provide clues to the diagenetic history of the carbonate under study. Chemically pure calcite normally shows blue CL, whilst Mn^{2+} is the primary activator and produces yellow-red emission. The presence of large amounts of Mn in skeletal

Table 1
δ¹³C and δ¹⁸O data, Cerro La Parva, with indication of lithostratigraphical unit, sample/subsample number, ammonite zones/subzones and age

Unit	Sample	Subsample	δ^{13}C (‰)	δ^{18}O (‰)	Ammonite zone/subzone	Age
Vaca Muerta Formation	1	a	1.81	−6.62	*Lissonia riveroi* zone	Early Valanginian
		b	1.08	−6.01	*Lissonia riveroi* zone	Early Valanginian
		c	0.54	−5.57	*Lissonia riveroi* zone	Early Valanginian
		d	1.78	−5.91	*Lissonia riveroi* zone	Early Valanginian
		e	2.43	−5.96	*Lissonia riveroi* zone	Early Valanginian
		f	1.58	−5.19	*Lissonia riveroi* zone	Early Valanginian
		g	1.07	−6.25	*Lissonia riveroi* zone	Early Valanginian
		h	1.48	−5.77	*Lissonia riveroi* zone	Early Valanginian
	4	a	2.09	−4.78	*Lissonia riveroi* zone	Early Valanginian
		b	1.82	−4.96	*Lissonia riveroi* zone	Early Valanginian
		c	1.30	−4.39	*Lissonia riveroi* zone	Early Valanginian
		d	2.17	−4.61	*Lissonia riveroi* zone	Early Valanginian
		e	1.87	−4.44	*Lissonia riveroi* zone	Early Valanginian
		f	1.71	−4.02	*Lissonia riveroi* zone	Early Valanginian
	11	a	3.02	−7.03	*Lissonia riveroi* zone	Early Valanginian
		b	2.49	−6.23	*Lissonia riveroi* zone	Early Valanginian
Mulichinco Formation	28	a	1.24	−5.58	*Olcostephanus atherstoni* subzone	Early Valanginian
		b	1.67	−4.91	*Olcostephanus atherstoni* subzone	Early Valanginian
		c	1.27	−5.17	*Olcostephanus atherstoni* subzone	Early Valanginian
		d	2.18	−4.47	*Olcostephanus atherstoni* subzone	Early Valanginian
	30	a1	0.71	−4.41	*Olcostephanus atherstoni* subzone	Early Valanginian
		a2	0.74	−4.28	*Olcostephanus atherstoni* subzone	Early Valanginian
		b	2.43	−3.55	*Olcostephanus atherstoni* subzone	Early Valanginian
		c	1.51	−4.48	*Olcostephanus atherstoni* subzone	Early Valanginian
		a3	0.66	−4.41	*Olcostephanus atherstoni* subzone	Early Valanginian
		d	2.44	−4.63	*Olcostephanus atherstoni* subzone	Early Valanginian
	31	a	2.80	−5.24	*Olcostephanus atherstoni* subzone	Early Valanginian
		b	3.45	−4.73	*Olcostephanus atherstoni* subzone	Early Valanginian
		c	2.78	−5.82	*Olcostephanus atherstoni* subzone	Early Valanginian
		d	2.14	−6.54	*Olcostephanus atherstoni* subzone	Early Valanginian
Agrio Formation − Pilmatué Member	32	a	2.75	−3.45	*Olcostephanus atherstoni* subzone	Early Valanginian
		b	2.92	−3.32	*Olcostephanus atherstoni* subzone	Early Valanginian
		c	1.48	−3.66	*Olcostephanus atherstoni* subzone	Early Valanginian
		d	2.53	−3.98	*Olcostephanus atherstoni* subzone	Early Valanginian
	33	b	2.10	−3.51	*Olcostephanus atherstoni* subzone	Early Valanginian
		c	2.09	−4.40	*Olcostephanus atherstoni* subzone	Early Valanginian
		d	2.83	−4.13	*Olcostephanus atherstoni* subzone	Early Valanginian
		e	1.66	−3.93	*Olcostephanus atherstoni* subzone	Early Valanginian
		f	2.09	−3.76	*Olcostephanus atherstoni* subzone	Early Valanginian
		f2	2.02	−3.81	*Olcostephanus atherstoni* subzone	Early Valanginian
		f3	2.20	−3.76	*Olcostephanus atherstoni* subzone	Early Valanginian
		a	1.97	−4.16	*Olcostephanus atherstoni* subzone	Early Valanginian
	37	a	1.86	−5.56	*Karakaschiceras attenuatum* subzone	Late Valanginian
		b	2.82	−4.35	*Karakaschiceras attenuatum* subzone	Late Valanginian
		c	2.81	−4.57	*Karakaschiceras attenuatum* subzone	Late Valanginian
		d	1.02	−6.45	*Karakaschiceras attenuatum* subzone	Late Valanginian
	38	a	1.66	−5.08	*Karakaschiceras attenuatum* subzone	Late Valanginian
		b	1.08	−7.31	*Karakaschiceras attenuatum* subzone	Late Valanginian
		c	2.04	−4.66	*Karakaschiceras attenuatum* subzone	Late Valanginian
		d	1.63	−6.61	*Karakaschiceras attenuatum* subzone	Late Valanginian
		e	3.13	−5.24	*Karakaschiceras attenuatum* subzone	Late Valanginian
		f1	2.88	−5.36	*Karakaschiceras attenuatum* subzone	Late Valanginian
		f2	2.87	−5.34	*Karakaschiceras attenuatum* subzone	Late Valanginian
		f3	3.08	−5.27	*Karakaschiceras attenuatum* subzone	Late Valanginian
	43	a	2.08	−3.46	*Karakaschiceras attenuatum* subzone	Late Valanginian
		b	0.89	−4.05	*Karakaschiceras attenuatum* subzone	Late Valanginian
		c	0.70	−3.36	*Karakaschiceras attenuatum* subzone	Late Valanginian
		d	1.76	−3.30	*Karakaschiceras attenuatum* subzone	Late Valanginian
		e	1.63	−5.22	*Karakaschiceras attenuatum* subzone	Late Valanginian
		f	2.12	−5.02	*Karakaschiceras attenuatum* subzone	Late Valanginian
	45	a1	2.80	−4.81	*Karakaschiceras attenuatum* subzone	Late Valanginian
		a2	2.58	−4.90	*Karakaschiceras attenuatum* subzone	Late Valanginian
		a3	2.81	−4.63	*Karakaschiceras attenuatum* subzone	Late Valanginian

Table 1 (*continued*)

Unit	Sample	Subsample	δ¹³C (‰)	δ¹⁸O (‰)	Ammonite zone/subzone	Age
		b	2.16	−4.13	*Karakaschiceras attenuatum* subzone	Late Valanginian
		c	3.39	−4.15	*Karakaschiceras attenuatum* subzone	Late Valanginian
		d	2.32	−3.30	*Karakaschiceras attenuatum* subzone	Late Valanginian
		e1	2.02	−3.14	*Karakaschiceras attenuatum* subzone	Late Valanginian
		e2	2.09	−4.08	*Karakaschiceras attenuatum* subzone	Late Valanginian
		e3	2.12	−4.09	*Karakaschiceras attenuatum* subzone	Late Valanginian
		f	2.41	−3.44	*Karakaschiceras attenuatum* subzone	Late Valanginian
		g	2.81	−3.16	*Karakaschiceras attenuatum* subzone	Late Valanginian
		h	2.52	−3.47	*Karakaschiceras attenuatum* subzone	Late Valanginian
	49	a	2.45	−3.73	*Karakaschiceras attenuatum* subzone	Late Valanginian
		b	2.34	−3.29	*Karakaschiceras attenuatum* subzone	Late Valanginian
		c	2.22	−4.32	*Karakaschiceras attenuatum* subzone	Late Valanginian
		d1	2.48	−4.16	*Karakaschiceras attenuatum* subzone	Late Valanginian
		d2	2.49	−4.18	*Karakaschiceras attenuatum* subzone	Late Valanginian
		d3	2.50	−4.13	*Karakaschiceras attenuatum* subzone	Late Valanginian

Table 2
δ¹³C and δ¹⁸O data from the Pilmatué Member of the Agrio Formation, Agua de la Mula, with indication of lithostratigrphical unit, sample/subsample number, ammonite zones/subzones and age

Unit	Sample	Subsample	δ¹³C (‰)	δ¹⁸O (‰)	Ammonite zone/subzone	Age
Agrio Formation	1	a	1.83	−4.32	*Pseudofavrella angulatiformis* subzone	Late Valanginian
− Pilmatué Member	6	a	1.49	−4.68	*Chacantuceras ornatum* subzone	Late Valanginian
	9	a	1.92	−4.86	*Chacantuceras ornatum* subzone	Late Valanginian
		b	1.82	−4.95	*Chacantuceras ornatum* subzone	Late Valanginian
		c	1.91	−4.92	*Chacantuceras ornatum* subzone	Late Valanginian
		d	2.03	−4.47	*Chacantuceras ornatum* subzone	Late Valanginian
	15	a	1.51	−4.26	*Neocomites sp.* subzone	latest Valanginian
		b	1.89	−4.28	*Neocomites sp.* subzone	latest Valanginian
		c	1.91	−3.71	*Neocomites sp.* subzone	latest Valanginian
		d	1.76	−3.48	*Neocomites sp.* subzone	latest Valanginian
	29	a	2.58	−2.66	*Neocomites sp.* subzone	latest Valanginian
		b	2.73	−2.70	*Neocomites sp.* subzone	latest Valanginian
		c	2.77	−2.61	*Neocomites sp.* subzone	latest Valanginian
		d	2.38	−2.86	*Neocomites sp.* subzone	latest Valanginian
	30	a	2.30	−2.56	*Neocomites sp.* subzone	latest Valanginian
		b	2.14	−2.53	*Neocomites sp.* subzone	latest Valanginian
	33	a	0.93	−3.32	*Holcoptychites neuquensis* subzone	Early Hauterivian
		b	1.23	−3.81	*Holcoptychites neuquensis* subzone	Early Hauterivian
	44	a	1.61	−4.55	*Holcoptychites neuquensis* subzone	Early Hauterivian
		b	2.03	−4.24	*Holcoptychites neuquensis* subzone	Early Hauterivian
	45	a	1.72	−2.53	*Holcoptychites agrioensis* subzone	Early Hauterivian
		b	1.43	−2.06	*Holcoptychites agrioensis* subzone	Early Hauterivian
	55	a	1.33	−2.64	*Holcoptychites agrioensis* subzone	Early Hauterivian
	63	a	2.28	−2.87	*Olcostephanus laticosta* subzone	Early Hauterivian
	76	a	1.58	−3.36	*Hoplitocrioceras gentilii* subzone	Early Hauterivian
	82	a	2.01	−3.03	*Hoplitocrioceras gentilii* subzone	Early Hauterivian
		b	2.65	−3.34	*Hoplitocrioceras gentilii* subzone	Early Hauterivian
		c	1.87	−3.02	*Hoplitocrioceras gentilii* subzone	Early Hauterivian
		d	1.86	−3.01	*Hoplitocrioceras gentilii* subzone	Early Hauterivian
	84	a	1.48	−3.76	*Hoplitocrioceras gentilii* subzone	Early Hauterivian
	90	a	1.52	−3.38	*Hoplitocrioceras gentilii* subzone	Early Hauterivian
		b	1.48	−3.40	*Hoplitocrioceras gentilii* subzone	Early Hauterivian
		c	2.02	−3.18	*Hoplitocrioceras gentilii* subzone	Early Hauterivian
		d	1.00	−3.51	*Hoplitocrioceras gentilii* subzone	Early Hauterivian
	92	a	2.44	−2.70	*Weavericeras vacaense* zone	Early Hauterivian
		b	3.00	−2.22	*Weavericeras vacaense* zone	Early Hauterivian
		c	3.03	−2.17	*Weavericeras vacaense* zone	Early Hauterivian
		d	3.09	−2.16	*Weavericeras vacaense* zone	Early Hauterivian
	93	a	1.90	−2.87	*Weavericeras vacaense* zone	Early Hauterivian
		b	−0.18	−2.66	*Weavericeras vacaense* zone	Early Hauterivian
		c	−0.10	−4.03	*Weavericeras vacaense* zone	Early Hauterivian
	94	a	−3.69	−5.53	*Weavericeras vacaense* zone	Early Hauterivian

Table 3
δ¹³C and δ¹⁸O data from the Agua de la Mula Member of the Agrio Formation, Agua de la Mula, with indication of lithostratigraphical unit, sample/subsample number, ammonite zones/subzones and age

Unit	Sample	Subsample	$\delta^{13}C$ (‰)	$\delta^{18}O$ (‰)	Ammonite zone/subzone	Age
Agrio Formation	1	1	0.04	−2.87	*Spitidiscus riccardii* zone	Late Hauterivian
– Agua de la Mula Member	9	9	0.65	−3.09	*Crioceratites schlagintweiti* zone	Late Hauterivian
	11	a	2.27	−1.93	*Crioceratites diamantensis* zone	Late Hauterivian
		b	2.23	−1.68	*Crioceratites diamantensis* zone	Late Hauterivian
		c	1.67	−2.17	*Crioceratites diamantensis* zone	Late Hauterivian
		d	1.89	−1.74	*Crioceratites diamantensis* zone	Late Hauterivian
		e	1.04	−2.37	*Crioceratites diamantensis* zone	Late Hauterivian
		f	1.83	−2.14	*Crioceratites diamantensis* zone	Late Hauterivian
	12	a	1.54	−1.53	*Crioceratites diamantensis* zone	Late Hauterivian
		b	2.27	−1.63	*Crioceratites diamantensis* zone	Late Hauterivian
		c	2.10	−1.60	*Crioceratites diamantensis* zone	Late Hauterivian
		d	0.73	−2.72	*Crioceratites diamantensis* zone	Late Hauterivian
		e	0.66	−2.07	*Crioceratites diamantensis* zone	Late Hauterivian
		f	1.91	−2.19	*Crioceratites diamantensis* zone	Late Hauterivian
		g	0.80	−2.19	*Crioceratites diamantensis* zone	Late Hauterivian
		h	0.91	−1.88	*Crioceratites diamantensis* zone	Late Hauterivian
		i	1.79	−1.84	*Crioceratites diamantensis* zone	Late Hauterivian
		j	1.23	−2.40	*Crioceratites diamantensis* zone	Late Hauterivian
	15	a	0.16	−2.38	*Crioceratites diamantensis* zone	Late Hauterivian
		b	−0.38	−2.06	*Crioceratites diamantensis* zone	Late Hauterivian
		c1	−0.31	−2.48	*Crioceratites diamantensis* zone	Late Hauterivian
		c2	−0.33	−2.52	*Crioceratites diamantensis* zone	Late Hauterivian
		c3	−0.27	−2.41	*Crioceratites diamantensis* zone	Late Hauterivian
		d	1.95	−2.25	*Crioceratites diamantensis* zone	Late Hauterivian
		e	1.90	−2.26	*Crioceratites diamantensis* zone	Late Hauterivian
		f	1.74	−2.37	*Crioceratites diamantensis* zone	Late Hauterivian
		g	1.65	−2.04	*Crioceratites diamantensis* zone	Late Hauterivian
		h	1.63	−1.53	*Crioceratites diamantensis* zone	Late Hauterivian
		i	1.04	−2.69	*Crioceratites diamantensis* zone	Late Hauterivian
		j1	0.84	−3.31	*Crioceratites diamantensis* zone	Late Hauterivian
		j2	0.79	−3.31	*Crioceratites diamantensis* zone	Late Hauterivian
		j3	0.96	−3.29	*Crioceratites diamantensis* zone	Late Hauterivian
	16	a	2.17	−2.70	*Crioceratites diamantensis* zone	Late Hauterivian
		b	1.87	−1.93	*Crioceratites diamantensis* zone	Late Hauterivian
		c	2.12	−2.32	*Crioceratites diamantensis* zone	Late Hauterivian
		d	−0.35	−2.07	*Crioceratites diamantensis* zone	Late Hauterivian
	19	a	1.16	−3.96	*Crioceratites diamantensis* zone	Late Hauterivian
		b	1.46	−1.70	*Crioceratites diamantensis* zone	Late Hauterivian
	20	a	2.02	−2.16	*Crioceratites diamantensis* zone	Late Hauterivian
	21	a	1.00	−4.71	*Crioceratites diamantensis* zone	Late Hauterivian
	22	a	1.27	−3.53	*Crioceratites diamantensis* zone	Late Hauterivian
	23	a	1.44	−3.53	*Crioceratites diamantensis* zone	Late Hauterivian
	24	a	1.67	−3.36	*Crioceratites diamantensis* zone	Late Hauterivian
	25	a	1.32	−3.30	*Crioceratites diamantensis* zone	Late Hauterivian
	28	a	2.22	−3.51	*Crioceratites diamantensis* zone	Late Hauterivian
	30	a	1.34	−3.66	*Crioceratites diamantensis* zone	Late Hauterivian
	31	31	1.61	−3.44	*Paraspiticeras groeberi* zone	Early Barremian
	33	b	1.66	−3.31	*Paraspiticeras groeberi* zone	Early Barremian
		a	2.11	−3.20	*Paraspiticeras groeberi* zone	Early Barremian
		2	0.63	−3.17	*Paraspiticeras groeberi* zone	Early Barremian
		4	2.65	−3.55	*Paraspiticeras groeberi* zone	Early Barremian
		10	1.19	−4.67	*Paraspiticeras groeberi* zone	Early Barremian
	36	b	2.36	−1.25	*Paraspiticeras groeberi* zone	Early Barremian
	37	37	−5.50	−3.29	*Paraspiticeras groeberi* zone	Early Barremian
	38	b	1.89	−1.39	*Paraspiticeras groeberi* zone	Early Barremian
		a	−0.23	−5.27	*Paraspiticeras groeberi* zone	Early Barremian
	40	1	2.07	−2.68	*Paraspiticeras groeberi* zone	Early Barremian
		2	1.03	−3.54	*Paraspiticeras groeberi* zone	Early Barremian
		2 rep	1.12	−3.51	*Paraspiticeras groeberi* zone	Early Barremian
		a	2.09	−1.81	*Paraspiticeras groeberi* zone	Early Barremian
		b	2.19	−2.54	*Paraspiticeras groeberi* zone	Early Barremian
		c1	2.36	−2.66	*Paraspiticeras groeberi* zone	Early Barremian
		c2	2.46	−2.70	*Paraspiticeras groeberi* zone	Early Barremian

Table 3 (*continued*)

Unit	Sample	Subsample	δ¹³C (‰)	δ¹⁸O (‰)	Ammonite zone/subzone	Age
		c3	2.31	−2.78	*Paraspiticeras groeberi* zone	Early Barremian
		d	1.77	−2.17	*Paraspiticeras groeberi* zone	Early Barremian
		e	1.92	−2.26	*Paraspiticeras groeberi* zone	Early Barremian
		f	1.42	−1.51	*Paraspiticeras groeberi* zone	Early Barremian
		3	1.21	−2.94	*Paraspiticeras groeberi* zone	Early Barremian

carbonates can be taken as an indicator of diagenetic alteration (e.g., Veizer, 1983; Marshall, 1992). The CL analysis described herein was performed using a Cambridge Image Technology cathodoluminescence CLMK4. Diagenetic alteration was not obvious by standard petrographic inspection. Under CL, most of the oysters were dully luminescent, whilst some growth bands adjacent to the shell margin, infilled microfractures, and the cement and sediment infilling borings were brightly luminescent (Fig. 3).

3.3. Sampling

In order to obtain sufficient shell carbonate for isotopic analysis, without compromise from diagenetically-altered
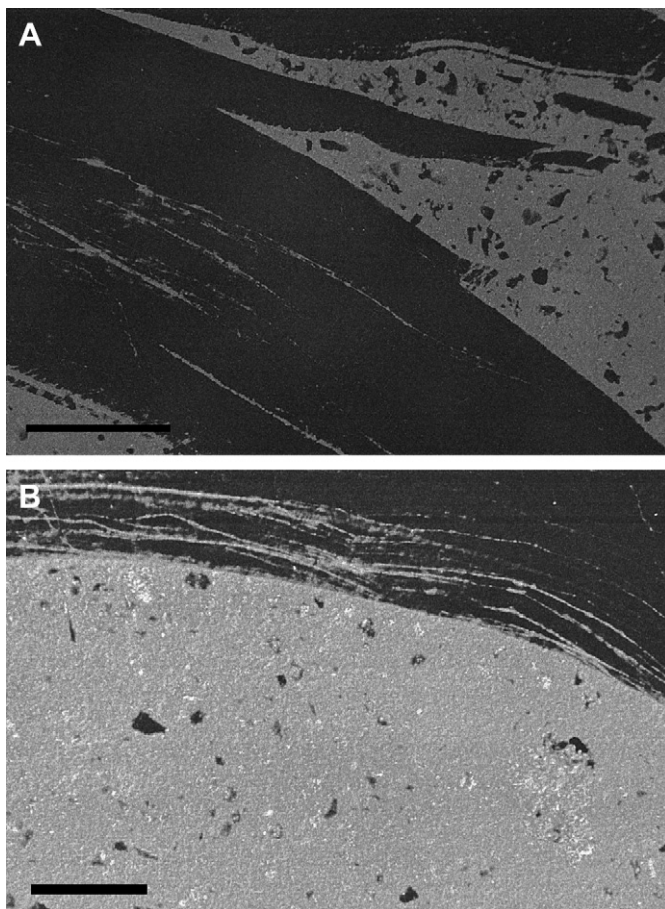

Fig. 3. A, Cathodoluminescence (CL) photomicrograph of oyster (Sample AM29 C7), showing a largely non-luminescent shell margin within a luminescent matrix. B, CL photomicrograph of oyster (Sample LP11 B), showing some luminescent growth bands (avoided during sampling) adjacent to the shell margin. Scale-bar = 2 mm in A and 1 mm in B.

areas of the oyster, each oyster was broken up with a vibrating microdrill. The external laminae (shown by CL to be diagenetically altered in some sample; Fig. 3) of the shell margins were discarded. By drilling at the edge of a broken shell, individual laminae broke away and could be isolated. These laminae were on average, 0.5 mm thick and up to 1 cm in diameter. Each lamina was washed in de-ionised water in an ultrasonic bath for five minutes. The core of each lamina was then drilled with a microdrill, avoiding fractured edges. Each drilled powder was analysed separately. Each oyster had between three and six samples taken in this way, depending on the total shell thickness and number of laminae.

3.4. Isotope analysis

The δ¹³C and δ¹⁸O values for oysters presented in this study were obtained using a GV Instruments Carbonate Acid Injector and GVI 2003 Mass Spectrometer, housed in the School of Planning, Architecture and Civil Engineering, Queen's University, Belfast. The δ¹³C and δ¹⁸O values obtained were calibrated against the internationally accepted International Atomic Energy Association carbonate standard NBS-19. Analytical reproducibility of the measurements is ±0.2 per mil based upon replicate analyses. The δ¹⁸O and δ¹³C data are reported in the conventional delta notation with respect to V-PDB (Figs. 4 and 5, Tables 1−3).

4. The δ¹³C and δ¹⁸O curves

The δ¹³C and δ¹⁸O curves are shown in Figs. 4−6, where each point represents the averaged data from each level and the error bars are 1 standard deviation. The lower part of the curve, derived from Cerro La Parva, is incomplete (Fig. 4), the gap representing the bulk of the Mulichinco Formation, which did not yield sufficient oysters. There are also some minor gaps in sampling higher in the succession. The δ¹³C curve shows several positive excursions of varying degrees of magnitude.

Within the Valanginian, the dark shales forming the top part of the Cerro La Parva succession show a shift to more positive δ¹³C values, consistently above 2.0‰. The excursion extends over much of the *Olcostephanus* (*O.*) *atherstoni* and *Karakaschiceras attenuatum* ammonite Subzones interval, which comprises a succession of black shales that is limited to the central part of the basin, west of Chos Malal. According to Aguirre-Urreta and Rawson (1997) and Aguirre-Urreta et al. (2005), the ammonite faunas of the *O.* (*O.*) *atherstoni-K. attenuatum* Subzones correlate with the bulk of the Mediterranean Province *Busnardoites campylotoxus* to *Saynoceras*
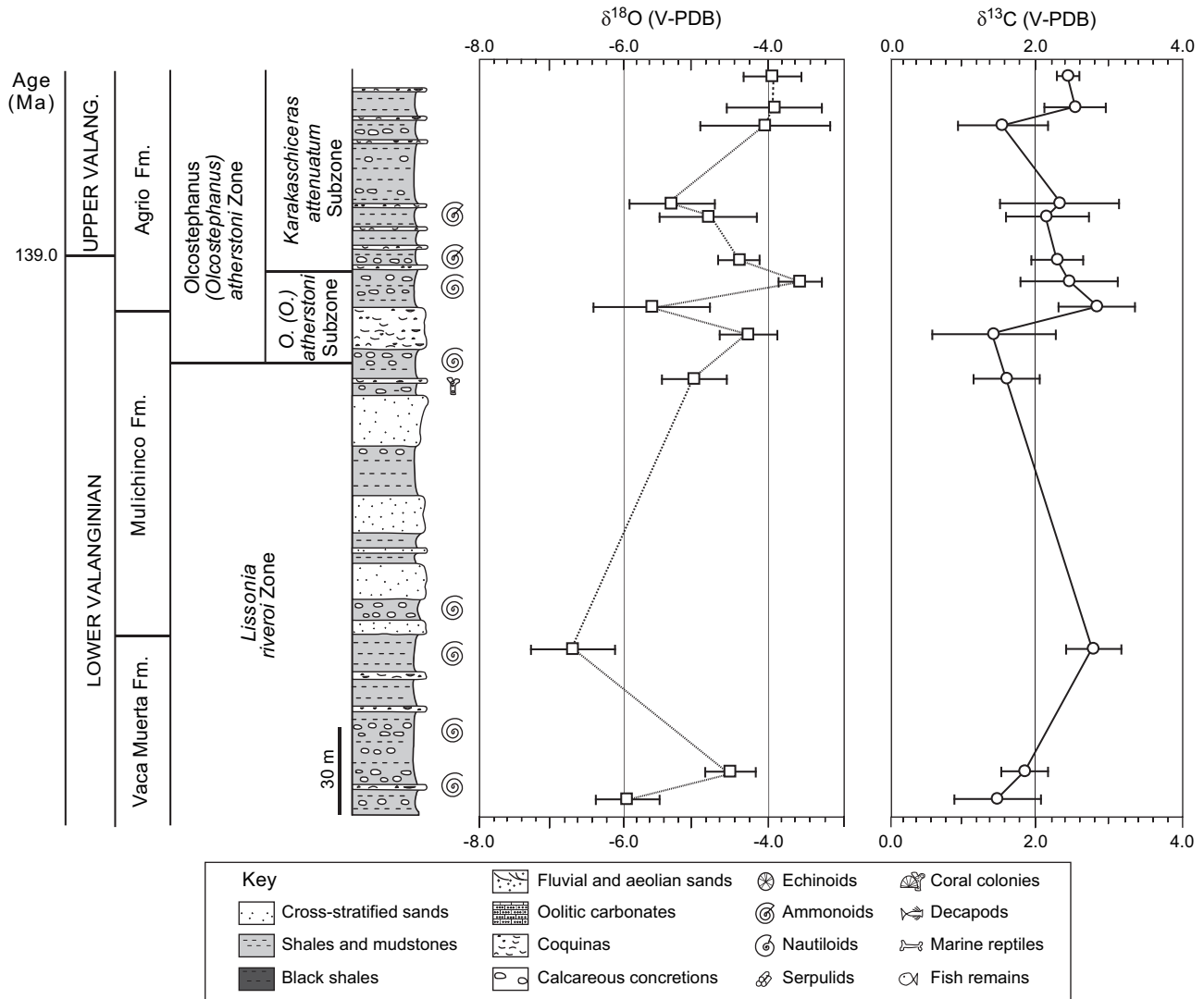
Fig. 4. Lithological log of the Cerro La Parva section, with lithostratigraphical and ammonite biostratigraphical correlations, and the δ^{13}C and δ^{18}O isotope curves. Each point represents the averaged data from each level and the error bars are 1 standard deviation. Numerical time-scale after Ogg et al. (2004).

verrucosum ammonite Zones, at which level the well-known mid-Valanginian positive carbon isotope excursion occurs (e.g., Weissert et al., 1998; Hennig et al., 1999; van de Schoot-brugge et al., 2000). The same event is also found at the correlative level in some boreal sequences (e.g., Price and Mutterlose, 2004).

Higher in the Valanginian, there is a brief excursion in the upper part of the *'Neocomites'* sp. ammonite Subzone, where black shales are again well developed. Ammonite correlations (Aguirre-Urreta et al., 2005) also indicate that the *Weaverice-ras vacaense* ammonite Zone may correlate with the *Lyticoce-ras nodosoplicatum* ammonite Zone in SE France, which contains a brief positive excursion in both the belemnite and bulk carbon curves (van de Schootbrugge et al., 2000). Within the Agua La Mula section, at the base of the *W. vacaense* Zone, there is a sharp facies change, from the underlying silty shales with thin sandstones in the upper part of the *Hoplitoc-rioceras gentilii* ammonite Subzone to black shales, but only a single data-point reveals more positive δ^{13}C values.

Negative oxygen isotope values are observed throughout the succession, ranging from approximately −7.0 to −1.3‰. Of note is that the most negative δ^{18}O values are seen from the lower part of the succession (*Lissonia riveroi -O.* (*O.*) *athe-rstoni* (Sub)zones), and are coincident with the most positive δ^{13}C values. These very negative δ^{18}O values, in conjunction with the degree of scatter shown in both carbon and oxygen data, are interpreted to indicate a fresh-water influence within the brachyhaline zone (Lazo et al., in press).

5. Discussion

Within the Neuquén Basin, major organic-rich units include the Upper Jurassic to Lower Cretaceous Vaca Muerta Forma-tion and the Pilmatué Member of the Agrio Formation (Ku-gler, 1985; Cruz et al., 1996; Tyson et al., 2005). The total organic carbon (TOC) content of the Vaca Muerta Formation decreases upwards, with the maximum TOC values (2–12 wt%) associated with the basal unit of the section (Kugler,
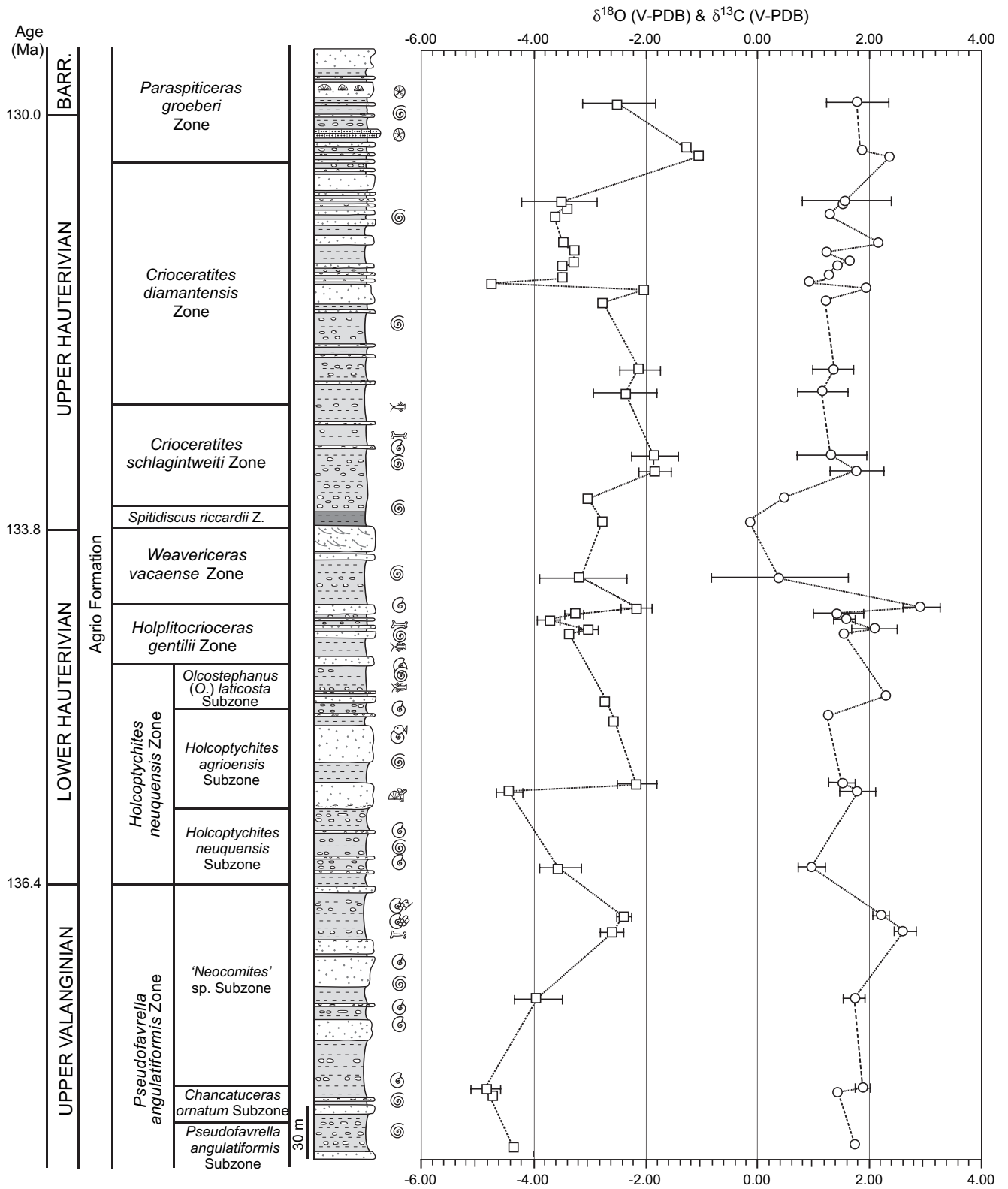
Fig. 5. Lithological log of the Agua La Mula section, with lithostratigraphical and ammonite biostratigraphical correlations, and the δ^{13}C and δ^{18}O isotope curves. Each point represents the averaged data from each horizon and the error bars are 1 standard deviation. For key see Fig. 4. Numerical time-scale after Ogg et al. (2004).
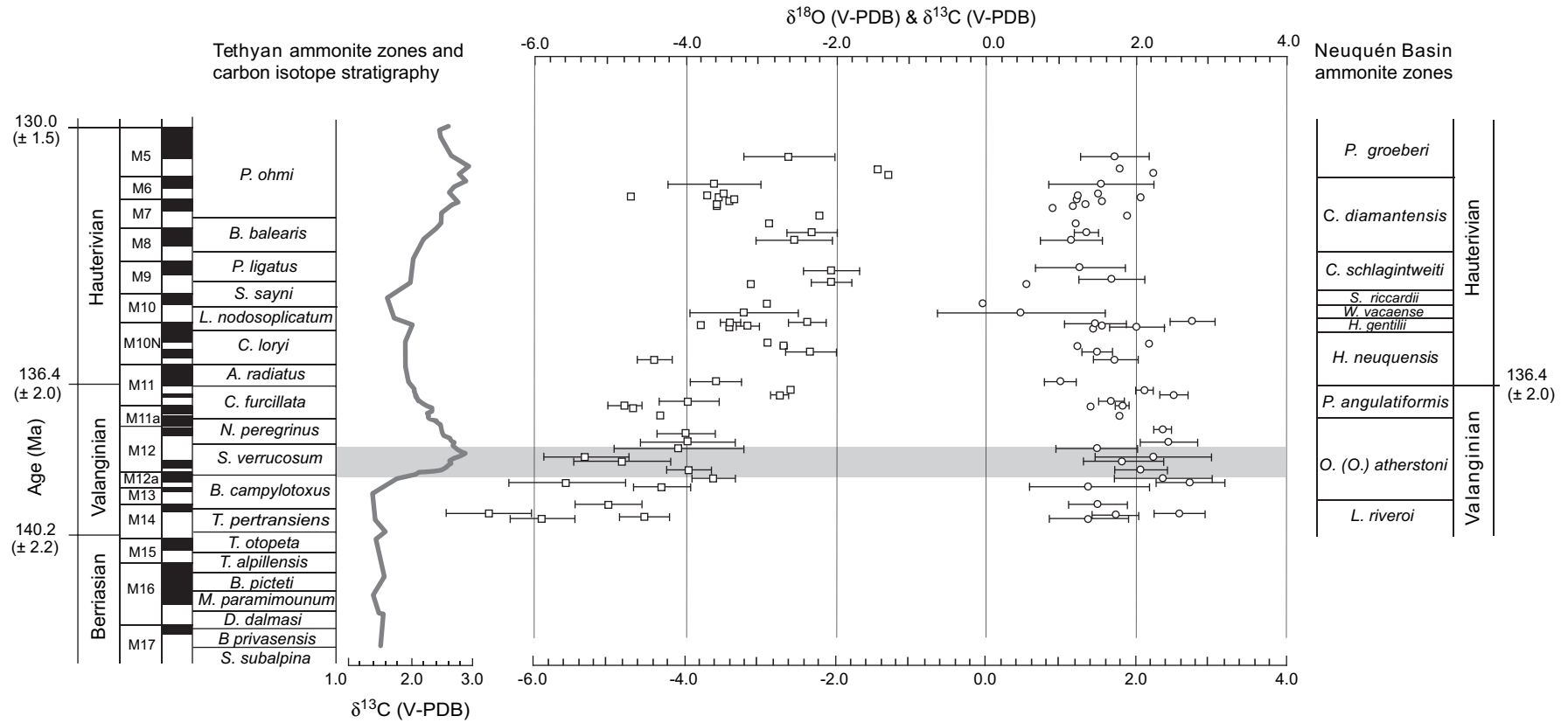
Fig. 6. Comparison of the Berriasian–Hauterivian composite Tethyan δ¹³C curve (from Weissert et al., 1998) and δ¹⁸O and δ¹³C isotope data from the Neuquén Basin. Sample positions are calibrated against ammonite zones and/or the stage boundary ages, assuming a constant sedimentation rate. Time-scale after Ogg et al. (2004), magnetostratigraphy from Channell and Erba (1992) and Tethyan ammonite zonation from Hoedemaeker et al. (2003).

1985; Scasso et al., 2005). Notably, Tyson et al. (2005) revealed both reasonably rich TOC concentrations (up to 7.4 wt%) and concentrations of type II/III organic matter (organic matter derived from algae, bacteria and marine zooplankton, with some higher plant contribution), from the base of the Pilmatué Member. The evidence presented here demonstrates that, in the Neuquén Basin, there may be a link between certain positive carbon isotope excursions and the accumulation of black 'organic-rich' shales. However, the data of Tyson et al. (2005) also show that higher TOC values are recorded from the *Spitidiscus* shale, coincident with the most negative carbon isotopes of this study. Hence, a simple relationship between carbon burial within the Neuquén Basin and positive carbon isotope excursions is not always apparent.

Ammonite correlations indicate that most of the observed carbon isotope excursions seen within the Neuquén Basin (Fig. 6) may correlate with excursions documented from the SE of France (Hennig et al., 1999; van de Schootbrugge et al., 2000). It is the mid-Valanginian excursion that has been recognised over much of the world and that has prompted much discussion over its origin. The excursion was first identified in a well-established time-scale by Lini et al. (1992). Since then it has been identified throughout the Tethyan area, and has subsequently been located in many other regions of the Northern Hemisphere (e.g., Bartolini, 2003; Price and Mutterlose, 2004). The $\delta^{13}C$ curves of the mid-Valanginian event (e.g., Weissert, 1989; Weissert et al., 1998; Lini et al., 1992) have typically been based upon bulk carbonate analyses. Within these studies, as each sample for isotopic analysis, in addition to nannofossil carbonate, may consist of a number of different components, including microspar, foraminiferal and molluscan shell micro-debris, this must lead to a dampening of the potential variation leading to an integrated $\delta^{13}C$ signal. Where individual faunal or floral components have been analysed across the Valanginian positive carbon isotope excursion (e.g., Price et al., 2000; van de Schootbrugge et al., 2000; Wortmann and Weissert, 2000; Price and Mutterlose, 2004; Gröcke et al., 2005) much greater variability is seen. It is therefore considered that the variations documented in the carbon record from the Neuquén Basin are genuine and reveal short-term fluctuations, possibly reflecting real and rapid changes in carbon cycling or local environmental conditions superimposed on the longer-term trend.

The origin of the mid-Valanginian excursion has been widely debated. It has been linked variously with global warming, volcanism and the widespread deposition of black shales. Lini et al. (1992) ascribed the positive carbon event to a greenhouse episode of the earth's climate. But comparison of $\delta^{13}C$ to proxy measurements of temperature, such as $\delta^{18}O$, Boreal-Tethyan floral and faunal distributions, glendonite nodules and possible glacial dropstones, provide abundant evidence of cool climatic conditions for much of the Valanginian and parts of the Hauterivian, partially contradicting the idea of Lini et al. (1992). Erba et al. (2004) found no palaeontological or $\delta^{18}O$ evidence of warming during the Valanginian oceanic anoxic event, and according to these authors, both nannofossils and oxygen isotopes record

a cooling event at the climax of the $\delta^{13}C$ excursion (see also Kessels et al., 2006).

Channell et al. (1993) linked the excursion to increased pCO_2 (the partial pressure of atmospheric CO_2) from volcanism, especially the Paraná-Etendeka continental flood-basalts. This link is problematic in its timing and origin (Courtillot et al., 1999), but Erba and Tremolada (2004) and Erba et al. (2004) concluded that these eruptions offer the best explanation for the excursion. Both these authors and Gröcke et al. (2005) suggested that such eruptions increased surface-water fertility, leading to localised black shale deposition, incursions of marine flora and fauna from other biotic areas, and increases in global weathering. The Paraná-Etendeka flood-basalts have been dated by Renne et al. (1992) and Ernesto et al. (1999). The ages obtained by $^{40}Ar/^{39}Ar$ analysis range between 133 and 130 Ma, indicating a very short-lived eruption for most of this large igneous province. Taking into consideration the geologic time-scale of the International Commission on Stratigraphy, the Valanginian ranges from 140.2 ± 3.0 to 136.4 ± 2.0 Ma (Ogg et al., 2004), thus ruling out any potential link between the mid-Valanginian positive $\delta^{13}C$ excursion and the flood-basalts of the Paraná-Etendeka Basin. It is recognised, however, that there are few reliable radiometric ages with precise stratigraphic controls within the Early Cretaceous (Ogg et al., 2004), and consequently there are large differences in ages between different timescales (cf. Channell et al., 1995a,b; Gradstein et al., 1995). If the Valanginian ages of Ogg etal. (2004) are used, the main volcanic activity occurred exclusively within the Late Hauterivian (for which time we have no evidence of a positive $\delta^{13}C$ shift in the Neuquén Basin). Therefore, another explanation is required for the positive $\delta^{13}C$ shift during the mid-Valanginian.

Gröcke et al. (2005), amongst others, reviewed the evidence for the relationship between the mid-Valanginian carbon isotope excursion and organic matter burial. They conclude that few black shales have been recorded in this interval. Although ODP Leg 198, drilled on Shatsky Rise, recovered pelagic sequences containing two organic-rich intervals (Site 1213; Shipboard Scientific Party, 2002), age constraints on these intervals, based upon shipboard results, preclude the determination of a possible temporal relationship with the mid-Valanginian $\delta^{13}C$ positive excursion (Brassell et al., 2004). However, as we demonstrate here, the Neuquén Basin sections show several discrete intervals of black shales linked with positive excursions, including the mid-Valanginian one.

6. Conclusions

The first carbon and oxygen isotope curves for the Valanginian to Early Barremian interval obtained from outcrops in the Neuquén Basin show carbon isotope excursions that are correlatable with ones documented from the Mediterranean region. An unequivocal relationship between $\delta^{13}C$ and organic matter burial for the mid-Valanginian has hitherto been less well documented than for other established oceanic anoxic events. This work redresses the lack of evidence of such a relationship, in that a number of major Lower Cretaceous units in the

Neuquén Basin, including the Vaca Muerta Formation and the Pilmatué Member of the Agrio Formation, are organic rich. It should be noted, however, that high TOC values recorded from the *Spitidiscus* shale coincide with the most negative carbon isotopes of this study, and for this reason, a straightforward relationship between carbon burial within the Neuquén Basin and positive carbon isotope excursions is not always apparent.

The dark shales forming the lowest beds of the Pilmatué Member at Cerro La Parva show the beginning of a $\delta^{13}C$ excursion that spans the mid-Valanginian *Olcostephanus* (*O.*) *atherstoni* and *Karakaschiceras attenuatum* ammonite Subzones. Therefore, within the Valanginian, it appears that burial of carbon may also have occurred outside of typical open-ocean marine settings, that is, in more marginal marine environments such as the Neuquén Basin.

Acknowledgements

References

Aguirre-Urreta, M.B., Rawson, P.F., 1997. The ammonite sequence in the Agrio Formation (Lower Cretaceous), Neuquén basin, Argentina. Geological Magazine 134, 449−458.

Aguirre-Urreta, M.B., Rawson, P.F., Concheyro, G.A., Bown, P.R., Ottone, E.G., 2005. Lower Cretaceous Biostratigraphy of the Neuquén Basin. In: Veiga, G.D., Spalletti, L.A., Howell, J.A., Schwarz, E. (Eds.), The Neuquén Basin, Argentina: a Case Study in Sequence Stratigraphy and Basin Dynamics. Geological Society, London, Special Publication 252, pp. 57−81.

Bartolini, A., 2003. Cretaceous radiolarian biochronology and carbon isotope stratigraphy of ODP Site 1149 (northwestern Pacific, Nadezhda Basin). In: Ludden, J.N., Plank, T., Escutia, C. (Eds.), Proceedings of the Ocean Drilling Program, Scientific Results 185. 185SR-011.

Brassell, S.C., Dumitrescu, M., ODP Leg 198 Shipboard Scientific Party, 2004. Recognition of alkenones in a Lower Aptian porcellanite from the west-central Pacific. Organic Geochemistry 35, 181−188.

Channell, J.E.T., Cecca, R., Erba, E., 1995a. Correlations of Hauterivian and Barremian (Early Cretaceous) stage boundaries to polarity chrons. Earth and Planetary Science Letters 134, 125−140.

Channell, J.E.T., Erba, E., Nakanishi, M.L., Tamaki, K., 1995b. Late Jurassic-Early Cretaceous time scales and oceanic magnetic anomaly block models. In: SEPM Special Publication 54, 51−63.

Channell, J.E.T., Erba, E., 1992. Early Cretaceous polarity chrons CM0 and CM11 recorded in northern Italian land sections near Brescia. Earth and Planetary Science Letters 108, 161−179.

Channell, J.E.T., Erba, E., Lini, A., 1993. Magnetostratigraphic calibration of the Late Valanginian carbon isotope event in pelagic limestones from Northern Italy and Switzerland. Earth and Planetary Science Letters 118, 145−166.

Cochran, J.K., Landman, N.H., Turekian, K.K., Michard, A., Scfarag, D.P., 2003. Paleoceanography of the Late Cretaceous (Maastrichtian) Western Interior Seaway of North America: evidence from Sr and O isotopes. Palaeogeography, Palaeoclimatology, Palaeoecology 191, 45−64.

Cooper, M.R., 1995. Exogyrid oysters (Bivalvia: Gryphaeoidea) from the Cretaceous of southeast Africa. Part 1. Durban Museum Novitates 20, 1−48.

Courtillot, V., Jaupart, C., Manighetti, I., Tapponnier, P., Besse, J., 1999. On causal links between flood basalts and continental breakup. Earth and Planetary Science Letters 166, 177−195.

Cruz, C.E., Villar, H.J., Muñoz, N., 1996. Los sistemas petroleros del Grupo Mendoza en la fosa de Chos Malal. Cuenca Neuquina. Argentina. XIII° Congreso Geológico Argentino y III° Congreso de Exploración de Hidro-carburos, Actas I, 45−60.

Doyle, P., Poiré, D.G., Spalletti, L.A., Pirrie, D., Brenchley, P., Matheos, S.D., 2005. Relative oxygenation of the Tithonian-Valanginian Vaca Muerta-Chachao formations of the Mendoza Shelf, Neuquén Basin, Argentina. In: Veiga, G.D., Spalletti, L.A., Howell, J.A., Schwarz, E. (Eds.), The Neuquén Basin, Argentina: a Case Study in Sequence Stratigraphy and Basin Dynamics. Geological Society, London, Special Publication 252, pp. 185−206.

Erba, E., Bartolini, A., Larson, R.L., 2004. Valanginian Weissert oceanic anoxic event. Geology 32, 149−152.

Erba, E., Tremolada, F., 2004. Nannofossil carbonate fluxes during the Early Cretaceous: phytoplankton response to nutrification episodes, atmospheric CO_2, and anoxia. Paleoceanography 19, PA1008. doi:10.1029/2003PA000884.

Ernesto, M., Raposoa, M.I.B., Marquese, L.S., Renne, P.R., Diogo, L.A., de Mine, A., 1999. Paleomagnetism, geochemistry and $^{40}Ar/^{39}Ar$ dating of the north-eastern Paraná Magmatic Province: tectonic implications. Journal of Geodynamics 28, 321−340.

Föllmi, K.B., Weissert, H., Bisping, M., Funk, H., 1994. Phosphogenesis, carbon-isotope stratigraphy, and platform evolution along the Lower Cretaceous northern Tethyan margin. Geological Society of America Bulletin 106, 729−746.

Gradstein, F.M., Agterberg, F.P., Ogg, J.G., Hardenbol, J., van Veen, P., Thierry, J., Huang, Z., 1995. A Triassic, Jurassic and Cretaceous timescale. In: Berggren, W.A., Kent, D.V., Aubry, M.-P., Hardenbol, J. (Eds.), Geochronology, Time Scales and Stratigraphic Correlation. SEPM Special Publication 54, pp. 95−128.

Gröcke, D.R., Price, G.D., Robinson, S.A., Baraboshkin, E., Ruffell, A.H., Mutterlose, J., 2005. The Valanginian (Early Cretaceous) positive carbon-isotope event recorded in terrestrial plants. Earth and Planetary Science Letters 240, 495−509.

Hennig, S., Weissert, H., Bulot, L., 1999. C-isotope stratigraphy, a calibration tool between ammonite- and magnetostratigraphy: the Valanginian-Hauterivian transition. Geologica Carpathica 50, 91−96.

Hoedemaeker, P.J., Reboulet, S., Aguirre-Urreta, M.B., Alsen, P., Aoutem, M., Atrops, F., Barragan, R., Company, M., González, C., Klein, J., Lukeneder, A., Ploch, I., Raisossadat, N., Rawson, P.F., Ropolo, P., Vasicek, Z., Vermeulen, J., Wippich, M.G.E., 2003. Report on the 1st International Workshop of the IUGS Lower Cretaceous Ammonite Working Group, the 'Kilian Group' (Lyon, 11 July 2002). Cretaceous Research 24, 89−94.

Holmden, C., Hudson, J.D., 2003. $^{87}Sr/^{86}Sr$ and Sr/Ca investigation of Jurassic mollusks from Scotland: implications for paleosalinities and the Sr/Ca ratio of seawater. Geological Society of America Bulletin 115, 1249−1264.

Jones, C.J., Jenkyns, H.C., Coe, A.L., Hesselbo, S., 1994. Strontium isotopic variations in Jurassic-Cretaceous seawater. Geochimica et Cosmochimica Acta 58, 3061−3074.

Kessels, K., Mutterlose, J., Michalzik, D., 2006. Early Cretaceous (Valanginian-Hauterivian) calcareous nannofossils and isotopes of the Northern Hemisphere: proxies for the understanding of Cretaceous climate. Lethaia 39, 157−172.

Kugler, R.L., 1985. Source rock characteristics, Los Molles and Vaca Muerta shales, Neuquén Basin, west-central Argentina. American Association of Petroleum Geologists Bulletin 69, 276.

Lazo, D.G., Aguirre-Urreta, M.B., Price, G.D., Rawson, P.F., Ruffell, A.H. Palaeosalinity variations in the Early Cretaceous of the Neuquén Basin, Argentina: evidence from oxygen isotopes and detailed palaeoecological analysis. Palaeogeography, Palaeoecology, in press.

Legarreta, L., Gulisano, C.A., 1989. Análisis estratigráfico secuencial de la cuenca Neuquina (Triásico Superior-Tereiario Inferior). In: Chebli, G.A., Spalletti, L.A. (Eds.), Cuencas Sedimentarias Argentinas. Serie Correlación Geológica 6, pp. 221–243.

Legarreta, L., Uliana, M.A., 1991. Jurassic-Cretaceous marine oscillations and geometry of back-arc basin fill, central Argentine Andes. Special Publications of the International Association of Sedimentologists 12, 429–450.

Lini, A., Weissert, H.L., Erba, E., 1992. The Valanginian carbon isotope event: a first episode of greenhouse climate conditions during the Cretaceous. Terra Nova 4, 374–384.

Marshall, J.D., 1992. Climatic and oceanographic isotopic signals from the carbonate rock record and their preservation. Geological Magazine 129, 143–160.

Ogg, J.G., Agterberg, F.P., Gradstein, F.M., 2004. The Cretaceous Period. In: Gradstein, F.M., Ogg, J.G., Smith, A.G. (Eds.), A Geologic Time Scale 2004. Cambridge University Press, Cambridge, pp. 344–383.

Price, G.D., Mutterlose, J., 2004. Isotopic signals from late Jurassic-early Cretaceous (Volgian-Valanginian) subArctic Belemnites, Yatria River, Western Siberia. Journal of the Geological Society, London 161, 959–968.

Price, G.D., Ruffell, A.H., Jones, C.E., Kalin, R.M., Mutterlose, J., 2000. Isotopic evidence for temperature variation during the Early Cretaceous (late Ryazanian-mid Hauterivian). Journal of the Geological Society, London 157, 335–343.

Renne, P.R., Ernesto, M., Pacca, I.G., Coe, R.S., Glen, J., Prévot, M., Perrin, M., 1992. Rapid eruption of the Paraná flood volcanics, rifting of southern Gondwanaland and the Jurassic-Cretaceous boundary. Science 258, 975–979.

Scasso, R.A., Alonso, M.S., Lanés, S., Villar, H.J., Laffitte, G., 2005. Geochemistry and petrology of a Middle Tithonian limestone-marl rhythmite in the Neuquén Basin, Argentina: depositional and burial history. In: Veiga, G.D., Spalletti, L.A., Howell, J.A., Schwarz, E. (Eds.), The Neuquén Basin, Argentina: a Case Study in Sequence Stratigraphy and Basin Dynamics. Geological Society, London, Special Publication 252, pp. 207–230.

van de Schootbrugge, B., Föllmi, K.B., Bulot, L.G., Burns, S.J., 2000. Paleoceanographic changes during the early Cretaceous (Valanginian-Hauterivian): evidence from oxygen and carbon stable isotopes. Earth and Planetary Science Letters 181, 15–31.

Shipboard Scientific Party, 2002. Leg 198 summary. In: Bralower, T.J., Premoli Silva, I., Malone, M.J., et al. (Eds.), Proceedings of the Ocean Drilling Program, Initial Reports 198. Ocean Drilling Program, College Station, TX, pp. 1–84.

Spalletti, L.A., Poire, D., Pirrie, D., Matheos, S., Doyle, P., 2001. Respuesta sedimentológica a cambios en el nivel de base en una secuencia mixta clástica-carbonática del Cretácico Inferior de la cuenca Neuquina, Argentina. Revista Sociedad Geológica de España 14, 57–74.

Steuber, T., Rauch, M., 2005. Evolution of the Mg/Ca ratio of Cretaceous seawater: implications from the composition of biological low-Mg calcite. Marine Geology 217, 199–213.

Tyson, R.V., Esherwood, P., Pattison, K.A., 2005. Organic facies variations in the Valanginian-mid-Hauterivian interval of the Agrio Formation (Chos Malal area, Neuquén, Argentina): local significance and global context. In: Veiga, G.D., Spalletti, L.A., Howell, J.A., Schwarz, E. (Eds.), The Neuquén Basin, Argentina: a Case Study in Sequence Stratigraphy and Basin Dynamics. Geological Society, London, Special Publication 252, pp. 251–266.

Uliana, M.A., Legarreta, L., 1993. Hydrocarbons habitat in a Triassic to Cretaceous Sub-Andean setting – Neuquén Basin, Argentina. Journal of Petroleum Geology 16, 397–420.

Veiga, G.D., Spalletti, L.A., Flint, S., 2002. Aeolian/fluvial interactions and high-resolution sequence stratigraphy of a non-marine lowstand wedge: the Avile Member of the Agrio Formation (Lower Cretaceous), central Neuquén Basin, Argentina. Sedimentology 49, 1001–1019.

Veizer, J., 1983. Chemical diagenesis of carbonates: theory and application of trace element technique. In: Arthur, M.A., et al. (Eds.), Stable Isotopes in Sedimentary Geology. SEPM Short Course 10, pp. 3.1–3.100.

Weissert, H., 1989. C-isotope stratigraphy, a monitor of paleoenvironmental change: a case study from the early Cretaceous. Surveys in Geophysics 10, 1–61.

Weissert, H., Lini, A., Föllmi, K.B., Kuhn, O., 1998. Correlation of Early Cretaceous carbon isotope stratigraphy and platform drowning events: a possible link? Palaeogeography, Palaeoclimatology, Palaeoecology 137, 189–203.

Wortmann, U.G., Weissert, H., 2000. Tying platform drowning to perturbations of the global carbon cycle with a δ^{13}C Org curve from the Valanginian of DSDP Site 416. Terra Nova 12, 289–294.